Design Sensitivity Analysis for Shape Optimization based on the Lie Derivative

Erin Kuci[a,b], François Henrotte[b,c], Pierre Duysinx[a], Christophe Geuzaine[b]

[a] *University of Liège, Department of Aerospace and Mechanical Engineering, Belgium*
[b] *University of Liège, Department of Electrical Engineering and Computer Science, Belgium*
[c] *Université catholique de Louvain, EPL-iMMC-MEMA, Belgium*

Abstract

The paper presents a theoretical framework for the shape sensitivity analysis of systems governed by partial differential equations. The proposed approach, based on geometrical concepts borrowed from differential geometry, shows that sensitivity of a performance function (i.e. any function of the solution of the problem) with respect to a given design variable can be represented mathematically as a Lie derivative, i.e. the derivative of that performance function along a flow representing the continuous shape modification of the geometrical model induced by the variation of the considered design variable. Theoretical formulae to express sensitivity analytically are demonstrated in detail in the paper, and applied to a nonlinear magnetostatic and a linear elastic problem, following both the direct and the adjoint approaches. Following the analytical approach, one linear system of which only the right-hand side needs be evaluated (the system matrix being known already) has to be solved for each of the design variables in the direct approach, or for each performance functions in the adjoint approach. A substantial gain in computation time is obtained this way compared to a finite difference evaluation of sensitivity, which requires solving a second nonlinear system for each design variable. This is the main motivation of the analytical approach. There is some freedom in the definition of the auxiliary flow that represents the shape modification. We present a method that makes benefit of this freedom to express sensitivity locally as a volume integral over a single layer of finite elements connected to both sides of the surfaces undergoing shape modification. All sensitivity calculations are checked with a finite difference in order to validate the analytic approach. Convergence is analyzed in 2D and 3D, with first and second order finite elements.

Keywords: Lie derivative, Shape Optimization, Adjoint method, Direct method, Velocity field, Elasticity, Magnetostatics

Contents

Email address: Erin.Kuci@ulg.ac.be (Erin Kuci)

1. Introduction

Shape optimization has been an active research area since the seminal work of Zienkiewicz et al. in the early 1970's [1, 2], which was aiming at determining the layout of a mechanical structure maximizing a performance measure under some design constraints. Shape optimization can however also be applied to systems governed by partial differential equations (PDEs), which introduces one extra level of difficulty. Methods for tackling such problems have been developed in the field of nonlinear mathematical programming since the early 1960's [3, 4, 5, 6]. In the most successful approaches, the original problem is approximated by a sequence of convex optimization subproblems that are explicit in the design variables, and that can be minimized effectively by relying on the derivative of the performance functions, e.g. through an interior point method [7], or a dual Lagrange maximization [5].

In this context, the concept of sensitivity is pivotal. Two approaches have emerged over the years. The first one differentiates the discretized algebraic system [8], whereas the second one acts as an analytical differentiation at the level of the variational formulation of the problem [9]. Sensitivity analysis has been developed so far mostly in the area of structural mechanics [10, 11, 12, 1, 13, 14, 15, 16]. Applications in other disciplines such as electromagnetics have also been proposed [17, 18, 19], but have been limited to problems expressed in terms of a scalar potential, leaving aside the problem of handling vector unknown fields, which requires a more general theoretical framework.

This generalized framework is the purpose of this paper. With the concept of Lie derivative [20, 21, 22, 23, 24], sensitivity is expressed analytically at the continuous level, prior to discretization. The Lie derivative is the derivative along a flow, and the flow considered here is a continuous modification of the geometrical domain as design variables variate. Several methods have been proposed to generate the velocity field of this flow, using either an isoparametric mapping [25, 26, 27, 28], the boundary displacement method [29, 30, 31], or the fictitious load method [32, 33]. In this paper, we propose a generic CAD-based mesh relocalization method for the computation of the velocity field, which is suited for shape optimization problems based on CAD representations and allows an efficient numerical implementation.

The paper is organized as follows. The optimization problem is posed in Section 2. Section 3 develops the theoretical aspects of sensitivity analysis based on differential geometry, and formulae to express Lie derivative practically are detailed in Section 4. Section 5 details the construction of the velocity field. In Sections 6 and 7, the general framework is used to derive analytical sensitivity formulas for various linear or nonlinear systems. The proposed approach is shown to give the same sensitivity formulas as [34] in the case of linear elastic problems, and to generalize to non-scalar fields the results established in [35, 36] for nonlinear magnetostatics.

2. Optimization Problem

Let us consider a bounded domain Ω whose regions are separated by interfaces $\gamma^{\boldsymbol{\tau}}$ undergoing shape modifications controlled by a set of design variables $\boldsymbol{\tau}$, Fig. 1. A physical problem is defined over Ω by a system of nonlinear PDEs expressed in terms of a state variable $\boldsymbol{z}$ and a design variable set $\boldsymbol{\tau}$. A weak formulation of this problem is obtained by, e.g., a Galerkin linearization approach, and can be written in a generic form

$$r(\boldsymbol{\tau}, \boldsymbol{z}^\star, \bar{\boldsymbol{z}}) = 0, \ \forall \bar{\boldsymbol{z}} \in Z_z^0, \tag{1}$$

with Z_z^0 an appropriate function space and $\boldsymbol{z}^\star$ the solution of the problem. The functional $r(\boldsymbol{\tau}, \boldsymbol{z}, \bar{\boldsymbol{z}})$ is called residual and is always linear with respect to $\bar{\boldsymbol{z}}$, i.e.

$$r(\boldsymbol{\tau}, \boldsymbol{z}, \boldsymbol{a} + \boldsymbol{b}) = r(\boldsymbol{\tau}, \boldsymbol{z}, \boldsymbol{a}) + r(\boldsymbol{\tau}, \boldsymbol{z}, \boldsymbol{b}).$$

The aim of a PDE-constrained shape optimization problem is to determine the geometric configuration $\boldsymbol{\tau}$ that minimizes a cost function $f_0(\boldsymbol{\tau}, \boldsymbol{z})$, subjected to m inequalities $f_j(\boldsymbol{\tau}, \boldsymbol{z}) \leq 0$, $j = 1, \ldots, m$, ensuring the manufacturability or the feasibility of the design. The design space is also limited by physical or technological side constraints $\tau_i^{min} \leq \tau_i \leq \tau_i^{max}$, $i = 1, \ldots, n$. Hence, the optimization problem reads

$$\begin{aligned} \min_{\boldsymbol{\tau}} \quad & f_0(\boldsymbol{\tau}, \boldsymbol{z}^\star) \\ s.t. \quad & f_j(\boldsymbol{\tau}, \boldsymbol{z}^\star) \leq 0, \ j = 1, \ldots, m \\ & \tau_i^{min} \leq \tau_i \leq \tau_i^{max}, \ i = 1, \ldots, n \\ & r(\boldsymbol{\tau}, \boldsymbol{z}^\star, \bar{\boldsymbol{z}}) = 0, \ \forall \bar{\boldsymbol{z}} \in Z_z^0. \end{aligned} \tag{2}$$

The evaluation of the performance functions f_0 and f_j for a given $\boldsymbol{\tau}$ requires the knowledge of $\boldsymbol{z}^\star$ for that particular value of $\boldsymbol{\tau}$, which implies solving anew

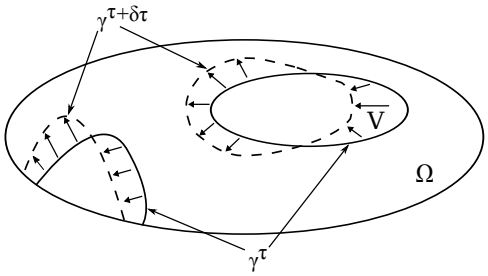

Figure 1: Considered domain Ω for a PDE-constrained shape optimization problem (2), where an interface γ^τ, parametrized by a design variable τ, is deformed onto $\gamma^{\tau+\delta\tau}$ as the design variable is perturbed by a small amount $\delta\tau$. The perturbation of the γ^τ generates a velocity field $\mathbf{v}$.

the nonlinear physical problem (1). The repetition of these evaluations is time-consuming for large scale applications.

The sensitivity matrix of problem (2) is the matrix

$$S_{ji} = \frac{\mathrm{d}f_j}{\mathrm{d}\tau_i}(\boldsymbol{\tau}, \boldsymbol{z}^\star) \tag{3}$$

of the derivatives of the performance functions with respect to the design variables. Optimization algorithms that do not rely on the sensitivity matrix necessitate a large number of function evaluations, and are therefore inefficient. Sensitivity-based algorithms, also often called gradient-based algorithms, on the other hand, offer a higher convergence rate, lesser function evaluations, and hence, in our case, limit the required number of resolutions of the finite element physical problem. In this article, a mathematical programming algorithm is used, coupled with a finite element analysis code [37, 38]. The optimization problem (2) is approximated by a series of convex subproblems explicit in the design variables, such as CONLIN [39] or MMA [40], which are then solved efficiently by a gradient-based primal, dual, or even combined primal-dual approach.

3. Design Sensitivity Analysis

We shall, for the sake of simplicity, consider one particular performance function, noted $f(\tau, \boldsymbol{z}^\star)$, and one particular design variable, noted τ. This amounts to deal with one particular component of the sensitivity matrix (3). The treatment of any other component would be identical.

3.1. Finite difference

The most straightforward approach approximates sensitivity with a simple finite difference [16]

$$\frac{\mathrm{d}f}{\mathrm{d}\tau}(\tau, \boldsymbol{z}^\star) \approx \frac{f\left(\tau + \delta\tau, \boldsymbol{z}^\dagger\right) - f\left(\tau, \boldsymbol{z}^\star\right)}{\delta\tau}, \tag{4}$$

where $\delta\tau$ is a small perturbation of the design variable. This evaluation requires solving two nonlinear problems on slightly different geometries to evaluate $\boldsymbol{z}^\star$

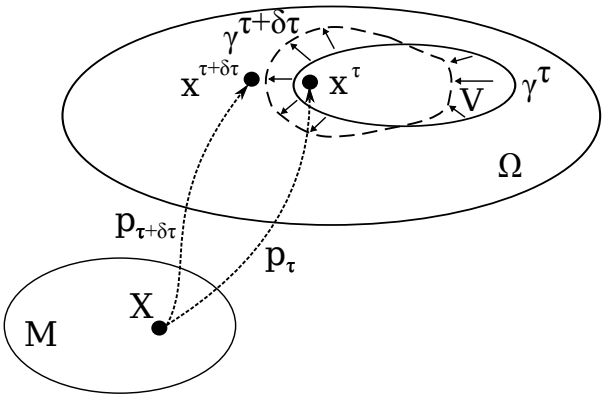

Figure 2: Considered material manifold M and Euclidean space Ω where the physical problem (1) is defined. Each geometrical configuration of Ω is characterized by an instance of the design variable τ, and represented by a smooth mapping p_τ (placement map) of each point $X \in M$ to each point $x^\tau \in \Omega$.

and $\boldsymbol{z}^\dagger$,

$$r(\tau, \boldsymbol{z}^\star, \bar{\boldsymbol{z}}) = 0, \ \forall \bar{\boldsymbol{z}} \in Z_z^0,$$
$$r(\tau + \delta\tau, \boldsymbol{z}^\dagger, \bar{\boldsymbol{z}}) = 0, \ \forall \bar{\boldsymbol{z}} \in Z_z^0,$$

of which only the first one is necessary and must be done in any case. The cost of the second one is indeed prohibitive considered that the sought sensitivity pertains to the linearization of the problem in the configuration corresponding to τ and $\boldsymbol{z}^\star$, and that this linearization has been done already to solve the first nonlinear problem. The finite difference approach is thus simple, but slow, and it is essentially used for validation purpose.

3.2. Analytical expression of sensitivity

It is more efficient to express the derivative of f with respect to τ analytically at a continuous level, prior to discretization. Writing the performance function explicitly in the form of an integral [1]

$$f(\tau, \boldsymbol{z}^\star) = \int_{\Omega(\tau)} F(\tau, \boldsymbol{z}^\star) \ \mathrm{d}\Omega, \tag{5}$$

sensitivity is the derivative with respect to τ of this integral and, in order to obtain an analytical expression, one has to be able to perform the differentiation under the integral sign.

The definition of the Lie derivative involves in this context a one parameter family of mappings

$$p_{\delta\tau} \ : \Omega(\tau) \subset E^3 \mapsto \Omega(\tau + \delta\tau) \subset E^3 \tag{6}$$

describing a smooth geometrical transformation of Ω in the Euclidean space E^3, with no tearing nor overlapping, that brings the interfaces between regions from

[1] If the performance function is a pointwise value, the expression of $F(\tau, \boldsymbol{z}^\star)$ will then involve a Dirac function.

their position γ^τ to their position $\gamma^{\tau+\delta\tau}$, Fig. 2. The mappings (6) with the scalar parameter $\delta\tau$ taking values in a neighborhood of zero and playing the role of a pseudo time variable, determines a flow on E^3 whose velocity field is noted $\mathbf{v}$. This velocity field plays a central role in the evaluation of the Lie derivative. An automatic procedure to build it in the general case is described in Section 5.

As the mappings (6) are invertible for all $\delta\tau$, tensor quantities (i.e. scalar fields, vector fields, or tensor fields) can be mapped back from $\Omega(\tau+\delta\tau)$ into $\Omega(\tau)$ using the inverse $p_{\delta\tau}^{-1}$ of $p_{\delta\tau}$. The Lie derivative of an arbitrary field ω in $\Omega(\tau)$ is then defined as

$$L_{\mathbf{v}}\omega = \lim_{\delta\tau\to 0} \frac{p_{\delta\tau}^{-1}\omega - \omega}{\delta\tau}, \tag{7}$$

where the index $\mathbf{v}$ in the notation $L_{\mathbf{v}}\omega$ makes reference to the velocity field characterizing the flow.

The Lie derivative is the mathematical concept describing the differentiation of an integral quantity over a deforming domain and verifies by definition the fundamental property

$$\frac{\mathrm{d}}{\mathrm{d}\tau}\int_{\Omega(\tau)} \omega = \int_{\Omega(\tau)} L_{\mathbf{v}}\omega. \tag{8}$$

Its properties and formulae to evaluate it practically are detailed in Section 4.

In particular, for the performance function (5) one can thus write

$$\frac{\mathrm{d}f}{\mathrm{d}\tau}(\tau, \boldsymbol{z}^\star) = \int_{\Omega(\tau)} L_{\mathbf{v}}F(\tau, \boldsymbol{z}^\star)\ \mathrm{d}\Omega. \tag{9}$$

By the chain rule of derivatives, the Lie derivative of the functional $F(\tau, \boldsymbol{z}^\star)$ has got two terms

$$L_{\mathbf{v}}F(\tau, \boldsymbol{z}^\star) = L_{\mathbf{v}}F(\tau, \boldsymbol{z}^\star)\Big|_{L_{\mathbf{v}}\boldsymbol{z}=0} + \big\{\mathrm{D}_{\boldsymbol{z}}F(\tau, \boldsymbol{z}^\star)\big\}\big(L_{\mathbf{v}}\boldsymbol{z}^\star\big). \tag{10}$$

The first term is the partial Lie derivative of the functional, defined as the Lie derivative holding the field argument $\boldsymbol{z}$ constant

$$D_\tau F(\tau, \boldsymbol{z}^\star) = L_{\mathbf{v}}F(\tau, \boldsymbol{z}^\star)\Big|_{L_{\mathbf{v}}\boldsymbol{z}=0}. \tag{11}$$

It accounts for changes in the value of the functional unrelated to the variation of the field. The second term involves the Fréchet derivative of the functional $F(\tau, \boldsymbol{z})$ with respect to its field argument $\boldsymbol{z}$. The Fréchet derivative is the linear operator $\big\{\mathrm{D}_{\boldsymbol{z}}F(\tau, \boldsymbol{z})\big\}\big(\,\cdot\,\big)$ defined by

$$\lim_{|\delta\boldsymbol{z}|\to 0} \frac{1}{|\delta\boldsymbol{z}|}\Big|F(\tau, \boldsymbol{z}+\delta\boldsymbol{z}) - F(\tau, \boldsymbol{z}) - \big\{\mathrm{D}_{\boldsymbol{z}}F(\tau, \boldsymbol{z})\big\}\big(\delta\boldsymbol{z}\big)\Big| = 0, \tag{12}$$

where the limit is taken over all sequences of non-zero $\delta\boldsymbol{z}$ that converge to zero. The arguments between parenthesis inside the curly braces indicate where the operator is evaluated, whereas the argument in between parenthesis outside the curly braces indicates to what the operator is applied. If the functional has several field arguments, a Fréchet derivative can be defined similarly for each of them.

3.3. Direct approach

We have shown in the previous section that sensitivity is expressed analytically

$$\frac{\mathrm{d}f}{\mathrm{d}\tau}(\tau, \boldsymbol{z}^\star) = \int_{\Omega(\tau)} \Big(D_\tau F(\tau, \boldsymbol{z}^\star) + \big\{ \mathrm{D}_{\boldsymbol{z}} F(\tau, \boldsymbol{z}^\star) \big\} \big(L_{\mathbf{v}} \boldsymbol{z}^\star \big) \Big) \, \mathrm{d}\Omega \tag{13}$$

in terms of $L_{\mathbf{v}} \boldsymbol{z}^\star$, which represents the evolution of the solution $\boldsymbol{z}^\star$ of the physical problem as the design parameter τ is changing. In order to determine this quantity, one states that the derivative of the residual (1) with respect to τ is zero in $\boldsymbol{z}^\star$,

$$\frac{\mathrm{d}}{\mathrm{d}\tau} r(\boldsymbol{\tau}, \boldsymbol{z}^\star, \bar{\boldsymbol{z}}) = 0, \ \forall \bar{\boldsymbol{z}} \in Z_z^0. \tag{14}$$

As the residual is an integral of the form

$$r(\tau, \boldsymbol{z}^\star, \bar{\boldsymbol{z}}) = \int_{\Omega(\tau)} R(\tau, \boldsymbol{z}^\star, \bar{\boldsymbol{z}}) \, \mathrm{d}\Omega, \tag{15}$$

the condition (14) is again the derivative of an integral. It can be treated in a similar fashion as the derivative of the performance function. By the chain rule of derivatives, one has

$$\begin{aligned} \frac{\mathrm{d}}{\mathrm{d}\tau} r(\tau, \boldsymbol{z}^\star, \bar{\boldsymbol{z}}) = \int_{\Omega(\tau)} \Big(& D_\tau R(\tau, \boldsymbol{z}^\star, \bar{\boldsymbol{z}}) + \big\{ \mathrm{D}_{\boldsymbol{z}} R(\tau, \boldsymbol{z}^\star, \bar{\boldsymbol{z}}) \big\} \big(L_{\mathbf{v}} \boldsymbol{z}^\star \big) \\ & + \big\{ \mathrm{D}_{\bar{\boldsymbol{z}}} R(\tau, \boldsymbol{z}^\star, \bar{\boldsymbol{z}}) \big\} \big(L_{\mathbf{v}} \bar{\boldsymbol{z}} \big) \Big) \, \mathrm{d}\Omega. \end{aligned} \tag{16}$$

The last term in the right-hand side of (16) vanishes, because linearity of $r(\tau, \boldsymbol{z}^\star, \bar{\boldsymbol{z}})$ with respect to its argument $\bar{\boldsymbol{z}}$ implies

$$\begin{aligned} \lim_{|\delta\bar{\boldsymbol{z}}| \to 0} \frac{1}{|\delta\bar{\boldsymbol{z}}|} \Big| R(\tau, \boldsymbol{z}, \bar{\boldsymbol{z}} + \delta\bar{\boldsymbol{z}}) - R(\tau, \boldsymbol{z}, \bar{\boldsymbol{z}}) - \big\{ \mathrm{D}_{\bar{\boldsymbol{z}}} R(\tau, \boldsymbol{z}, \bar{\boldsymbol{z}}) \big\} \big(\delta\bar{\boldsymbol{z}} \big) \Big| = \\ \lim_{|\delta\bar{\boldsymbol{z}}| \to 0} \frac{1}{|\delta\bar{\boldsymbol{z}}|} \Big| R(\tau, \boldsymbol{z}, \delta\bar{\boldsymbol{z}}) - \big\{ \mathrm{D}_{\bar{\boldsymbol{z}}} R(\tau, \boldsymbol{z}, \bar{\boldsymbol{z}}) \big\} \big(\delta\bar{\boldsymbol{z}} \big) \Big| = 0. \end{aligned}$$

Hence the identity

$$\big\{ \mathrm{D}_{\bar{\boldsymbol{z}}} R(\tau, \boldsymbol{z}, \bar{\boldsymbol{z}}) \big\} \big(\delta\bar{\boldsymbol{z}} \big) = R(\tau, \boldsymbol{z}, \delta\bar{\boldsymbol{z}}), \tag{17}$$

and in particular, for $\boldsymbol{z} = \boldsymbol{z}^\star$, $\delta\bar{\boldsymbol{z}} = L_{\mathbf{v}} \bar{\boldsymbol{z}}$ and using (1),

$$\int_{\Omega(\tau)} \big\{ \mathrm{D}_{\bar{\boldsymbol{z}}} R(\tau, \boldsymbol{z}^\star, \bar{\boldsymbol{z}}) \big\} \big(L_{\mathbf{v}} \bar{\boldsymbol{z}} \big) \, \mathrm{d}\Omega = r(\tau, \boldsymbol{z}^\star, L_{\mathbf{v}} \bar{\boldsymbol{z}}) = 0. \tag{18}$$

The left-hand side of (16) being zero, one has finally

$$\int_{\Omega(\tau)} \Big(D_\tau R(\tau, \boldsymbol{z}^\star, \bar{\boldsymbol{z}}) + \big\{ \mathrm{D}_{\boldsymbol{z}} R(\tau, \boldsymbol{z}^\star, \bar{\boldsymbol{z}}) \big\} \big(L_{\mathbf{v}} \boldsymbol{z}^\star \big) \Big) \, \mathrm{d}\Omega = 0, \ \forall \bar{\boldsymbol{z}} \in Z_z^0, \tag{19}$$

which is the sought weak form of a linear problem allowing to solve for $L_{\mathbf{v}} \boldsymbol{z}^\star$.

The Fréchet derivative term in (19) involves the tangent stiffness matrix of the nonlinear problem (1), and hence, in practice, the jacobian matrix of the problem after finite element discretization and convergence of the iterative

nonlinear process. This term is therefore already known from the finite element solving, and needs not be recomputed when solving (19). The partial Lie derivative in (19) accounts for the explicit dependency (i.e. holding the field argument constant) of the residual on the variation of τ. It is the right-hand side of the system determining $L_{\mathbf{v}}\boldsymbol{z}^\star$, which can also be evaluated analytically. The *semi-analytic approach* [41], however, consists in evaluating this term by a finite difference. Finite difference is done at a moderate numerical cost here, as $\boldsymbol{z}^\star$ is already known and $\boldsymbol{z}^\dagger$ is not needed.

3.4. Adjoint approach

An alternative to the method of previous section that solves explicitly for $L_{\mathbf{v}}\boldsymbol{z}^\star$ is the adjoint approach. The idea is to define an auxiliary performance function, called augmented Lagrangian function,

$$\bar{f}(\tau,\boldsymbol{z},\boldsymbol{\lambda}) = f(\tau,\boldsymbol{z}) - r(\tau,\boldsymbol{z},\boldsymbol{\lambda}) = \int_{\Omega(\tau)} \Big(F(\tau,\boldsymbol{z}^\star) - R(\tau,\boldsymbol{z}^\star,\boldsymbol{\lambda})\Big)\ \mathrm{d}\Omega, \tag{20}$$

with $\boldsymbol{\lambda}$ a Lagrange multiplier. As (1) implies that the residual $r(\tau,\boldsymbol{z}^\star,\lambda)$ is zero at equilibrium, one has

$$\bar{f}(\tau,\boldsymbol{z}^\star,\boldsymbol{\lambda}) = f(\tau,\boldsymbol{z}^\star), \tag{21}$$

and the sensitivity is expressed in terms of the auxiliary performance function $\bar{f}$ by

$$\frac{\mathrm{d}f}{\mathrm{d}\tau}(\tau,\boldsymbol{z}^\star) = \frac{\mathrm{d}\bar{f}}{\mathrm{d}\tau}(\tau,\boldsymbol{z}^\star,\boldsymbol{\lambda}). \tag{22}$$

Differentiation of (20) with respect to τ yields

$$\begin{aligned}\frac{\mathrm{d}\bar{f}}{\mathrm{d}\tau}(\tau,\boldsymbol{z}^\star,\boldsymbol{\lambda}) = \int_{\Omega(\tau)} \Big(&D_\tau F(\tau,\boldsymbol{z}^\star) - D_\tau R(\tau,\boldsymbol{z}^\star,\boldsymbol{\lambda}) \\ &+ \big\{\mathrm{D}_{\boldsymbol{z}} F(\tau,\boldsymbol{z}^\star)\big\}\big(L_{\mathbf{v}}\boldsymbol{z}^\star\big) - \big\{\mathrm{D}_{\boldsymbol{z}} R(\tau,\boldsymbol{z}^\star,\boldsymbol{\lambda})\big\}\big(L_{\mathbf{v}}\boldsymbol{z}^\star\big)\Big)\ \mathrm{d}\Omega,\end{aligned} \tag{23}$$

where we have already omitted the null term (18).

Let now $\boldsymbol{\lambda}^\star$ be the solution of the so-called adjoint problem

$$\int_{\Omega(\tau)} \Big(\big\{\mathrm{D}_{\boldsymbol{z}} F(\tau,\boldsymbol{z}^\star)\big\}\big(\bar{\boldsymbol{\lambda}}\big) - \big\{\mathrm{D}_{\boldsymbol{z}} R(\tau,\boldsymbol{z}^\star,\boldsymbol{\lambda}^\star)\big\}\big(\bar{\boldsymbol{\lambda}}\big)\Big)\ \mathrm{d}\Omega = 0,\ \forall \bar{\boldsymbol{\lambda}} \in Z_{\boldsymbol{\lambda}}. \tag{24}$$

As (24) holds for $\bar{\boldsymbol{\lambda}} = L_{\mathbf{v}}\boldsymbol{z}^\star \in Z_{\boldsymbol{\lambda}}$, and has the identity

$$\int_{\Omega(\tau)} \Big(\big\{\mathrm{D}_{\boldsymbol{z}} F(\tau,\boldsymbol{z}^\star)\big\}\big(L_{\mathbf{v}}\boldsymbol{z}^\star\big) - \big\{\mathrm{D}_{\boldsymbol{z}} R(\tau,\boldsymbol{z}^\star,\boldsymbol{\lambda}^\star)\big\}\big(L_{\mathbf{v}}\boldsymbol{z}^\star\big)\Big)\ \mathrm{d}\Omega = 0, \tag{25}$$

and the last two terms in the right-hand side of (23) cancel out each other if $\boldsymbol{\lambda} = \boldsymbol{\lambda}^\star$. Sensitivity is then given by

$$\frac{\mathrm{d}\bar{f}}{\mathrm{d}\tau}(\tau,\boldsymbol{z}^\star,\boldsymbol{\lambda}^\star) = \int_{\Omega(\tau)} \Big(D_\tau F(\tau,\boldsymbol{z}^\star) - D_\tau R(\tau,\boldsymbol{z}^\star,\boldsymbol{\lambda})\Big)\ \mathrm{d}\Omega, \tag{26}$$

in terms of the solutions of the nonlinear problem (1) and of the adjoint problem (24).

The system matrix of adjoint problem (24) is again the tangent stiffness matrix of the nonlinear problem (1), i.e. the jacobian matrix after finite element discretization and convergence of the iterative nonlinear process. It can be reused if the same discretization is used for solving (24) and (1).

3.5. Discussion

The direct and the adjoint methods are now compared to determine in which conditions one has to favor one over the other.

Assuming a discretization $\boldsymbol{z} = \sum_{p=1}^{N} z_p \boldsymbol{w}_p$ of the unknown field, with basis functions $\boldsymbol{w}_p \in Z_z^0$ and N the number of nodal unknowns, one solves with the direct method the linear problem (19), which is of the form

$$\sum_{q=1}^{N} J_{pq}^{\star}\, x_q = b_p, \tag{27}$$

with

$$J_{pq}^{\star} = \big\{ \mathrm{D}_{\boldsymbol{z}} R(\tau, \boldsymbol{z}^{\star}, \boldsymbol{w}_p) \big\} \big(\boldsymbol{w}_q \big) \tag{28}$$

the component of the nonlinear physical problem (1) jacobian matrix, and

$$b_p = D_{\tau} R(\tau, \boldsymbol{z}^{\star}, \boldsymbol{w}_p) \tag{29}$$

the fictitious load proper to the design variable τ, representing the partial Lie derivative of the residual associated with the test function $\bar{\boldsymbol{z}} \equiv \boldsymbol{w}_p$. One has a vector b_p for each design variable τ, and thus n linear systems like (27) to solve in a system with n design variables. Both $J_{pq}^{\star}$ and b_p are evaluated for $\boldsymbol{z} = \boldsymbol{z}^{\star}$, i.e., for the converged solution of the nonlinear iterative process. The matrix $J_{pq}^{\star}$ is thus known from the solving of (1) and needs not be recomputed.

The solution of (27), which is the field $\sum_{p=1}^{N} x_p \boldsymbol{w}_p \equiv L_{\mathbf{v}} \boldsymbol{z}^{\star}$, is a discrete estimation of the derivative of the solution $\boldsymbol{z}^{\star}$ of (1) with respect to the design variable τ or, put in a more accurate way, of the Lie derivative of $\boldsymbol{z}^{\star}$ along the flow associated with the variation of τ. This field is exactly what is needed to evaluate the sensitivity of the performance function with respect to τ

$$\frac{\mathrm{d}f}{\mathrm{d}\tau}(\tau, \boldsymbol{z}^{\star}) = \int_{\Omega(\tau)} \Big(D_{\tau} F(\tau, \boldsymbol{z}^{\star}) + \big\{ \mathrm{D}_{\boldsymbol{z}} F(\tau, \boldsymbol{z}^{\star}) \big\} \big(x_p \boldsymbol{w}_p \big) \Big)\, \mathrm{d}\Omega, \tag{30}$$

since the performance function f being known (5), its Fréchet derivative $\mathrm{D}_{\boldsymbol{z}} F$ and its partial Lie derivative $D_{\tau} F$ can both be expressed analytically.

With the adjoint approach, a system like (27) is also solved, with $J_{pq}^{\star}$ again given by (28), and

$$b_p = \big\{ \mathrm{D}_{\boldsymbol{z}} F(\tau, \boldsymbol{z}^{\star}) \big\} \big(\boldsymbol{w}_p \big) \tag{31}$$

the adjoint load proper to the performance function f. The solution of the system, $\sum_{p=1}^{N} x_p \boldsymbol{w}_p \equiv \boldsymbol{\lambda}^{\star} \in Z_{\boldsymbol{\lambda}}$, is now the so-called adjoint field, in terms of which the sensitivity of the performance function with respect to τ is expressed as

$$\frac{\mathrm{d}f}{\mathrm{d}\tau}(\tau, \boldsymbol{z}^{\star}) = \int_{\Omega(\tau)} \Big(D_{\tau} F(\tau, \boldsymbol{z}^{\star}) - D_{\tau} R(\tau, \boldsymbol{z}^{\star}, \boldsymbol{\lambda}) \Big)\, \mathrm{d}\Omega. \tag{32}$$

The first term is identical to that in (30), and the second term implies an evaluation of the partial Lie derivative of the residual of the problem (1) with the adjoint field $\boldsymbol{\lambda}^{\star}$ as test function $\bar{\boldsymbol{z}}$. One has also a vector b_p for each performance function f, and thus m linear systems like (27) to solve in a system with m performance functions.

Both the direct and the adjoint approaches require solving the nonlinear system (1), in order to determine the solution $\boldsymbol{z}^{\star}$ corresponding to the selected

design variables $\boldsymbol{\tau}$. One has then to solve one linear system for each of the n design variables in the direct approach, or alternatively one linear system for each of the m performance functions in the adjoint approach. This is in both cases a clear performance advantage compared to the finite difference approach, for which a nonlinear problem like (1) has to be solved for each design variable. The direct method should be preferred when the number of performance functions exceeds the number of design variables, $m > n$, otherwise the adjoint method is preferable.

4. Lie derivative formula sheet

Lie derivatives are playing an important role in the analytical expression of sensitivity. We now present formulae to evaluate the Lie derivative of scalar, vector and tensor fields. The purpose of this paper is however not to give a complete mathematical derivation of this, but rather to provide engineers and practitioners in the field of optimization with a useful formula sheet. We therefore stick with standard vector and tensor analysis notations and give a number of results without proof.

The Lie derivative verifies the Leibniz rule for scalar fields

$$L_{\mathbf{v}}(fg) = (L_{\mathbf{v}}f)g + f(L_{\mathbf{v}}g), \tag{33}$$

vector fields

$$L_{\mathbf{v}}(\boldsymbol{F}\cdot\boldsymbol{G}) = (L_{\mathbf{v}}\boldsymbol{F})\cdot\boldsymbol{G} + \boldsymbol{F}\cdot(L_{\mathbf{v}}\boldsymbol{G}), \tag{34}$$

and tensor fields

$$L_{\mathbf{v}}(A:B) = (L_{\mathbf{v}}A):B + A:(L_{\mathbf{v}}B), \tag{35}$$

where the colon : stands for the tensor product, $A : B = A_{ij}B_{ij}$ (implicit summation assumed on repeated indices in all the paper).

The Lie derivative of a scalar function f is

$$L_{\mathbf{v}}f = \frac{\partial f}{\partial \tau} + \mathbf{v}^T\nabla f, \tag{36}$$

with $\mathbf{v}$ the velocity field characterizing the flow. This is the classical expression for the convective derivative of a scalar quantity.

The Lie derivative of vector fields is more delicate. There exist several geometrical objects that have three components in an Euclidean space, but behaving differently under transformations like (6). Besides genuine vector fields, which convey the idea of motion and trajectory (e.g. the velocity $\mathbf{v}$ or displacement $\boldsymbol{u}$ fields), we have to deal with circulation densities (also called 1-forms), which are quantities that make sense when integrated over a curve, and whose tangential component is continuous at material interfaces (e.g. the magnetic vector potential $\boldsymbol{A}$ or the magnetic field $\boldsymbol{H}$) and flux densities (2-forms), which are quantities that make sense when integrated over a surface, and whose normal component is continuous at material interfaces (e.g. the flux density $\boldsymbol{B}$ and the current density $\boldsymbol{J}$). Although genuine vector fields, circulation densities and flux densities can be indiscriminately regarded as vector fields in an Euclidean space, their Lie derivative are different under the transformation (6) and they must therefore be carefully distinguished when evaluating the Lie derivative of an

expression involving such objets. The Lie derivative of a vector field $\boldsymbol{W} = W_i \boldsymbol{e}_i$ reads

$$L_{\mathbf{v}} \boldsymbol{W} = (L_{\mathbf{v}} W_i) \boldsymbol{e}_i - (\nabla \mathbf{v})^{\mathbf{T}} \boldsymbol{W}, \tag{37}$$

whereas that of a 1-form $\boldsymbol{H} = H_i \boldsymbol{e}_i$ reads

$$L_{\mathbf{v}} \boldsymbol{H} = (L_{\mathbf{v}} H_i) \boldsymbol{e}_i + (\nabla \mathbf{v}) \boldsymbol{H}, \tag{38}$$

and that of a 2-form $\boldsymbol{B} = B_i \boldsymbol{e}_i$

$$L_{\mathbf{v}} \boldsymbol{B} = (L_{\mathbf{v}} B_i) \boldsymbol{e}_i - (\nabla \mathbf{v})^{\mathbf{T}} \boldsymbol{B} + \boldsymbol{B} \operatorname{div} \mathbf{v} \tag{39}$$

in an orthonormal basis $\{\boldsymbol{e}_i, i = 1, 2, 3\}$ and with the notations

$$\begin{aligned}
(\nabla \mathbf{v}) &= (\nabla \mathbf{v})_{kj} \ \boldsymbol{e}_k \boldsymbol{e}_j^T = \frac{\partial V_j}{\partial x_k} \ \boldsymbol{e}_k \boldsymbol{e}_j^T \\
(\nabla \mathbf{v})^T &= \frac{\partial V_j}{\partial x_k} \ \boldsymbol{e}_j \boldsymbol{e}_k^T \\
(\nabla \mathbf{v}) \boldsymbol{e}_i &= \frac{\partial V_i}{\partial x_k} \ \boldsymbol{e}_k \\
(\nabla \mathbf{v})^T \boldsymbol{e}_i &= \frac{\partial V_j}{\partial x_i} \ \boldsymbol{e}_j \\
(\nabla \mathbf{v}) \boldsymbol{F} &= \frac{\partial V_i}{\partial x_k} F_i \ \boldsymbol{e}_k \\
(\nabla \mathbf{v})^T \boldsymbol{F} &= \frac{\partial V_j}{\partial x_i} F_i \ \boldsymbol{e}_j \\
\operatorname{div} \mathbf{v} &= \partial V_i / \partial x_i = \operatorname{tr}(\nabla \mathbf{v}) \\
A : B &= A_{ij} B_{ij} \\
\boldsymbol{e}_i \boldsymbol{e}_j^T : \boldsymbol{e}_p \boldsymbol{e}_q^T &= \delta_{ip} \delta_{jq}.
\end{aligned}$$

We shall only use (38) and (39) in the expression of sensitivity.

The Lie derivative of a material law like $\boldsymbol{H}(\boldsymbol{B})$ is the Lie derivative of a functional (a function of a field quantity) instead of the derivative of a field. It is treated as follows. First, the material law must be regarded as a relationship between the components of the fields

$$H_i(B_k) = \nu_{ij} B_j, \tag{40}$$

with ν_{ij} the components of the nonlinear reluctivity tensor of the material. Taking the Lie derivative yields

$$\begin{aligned}
L_{\mathbf{v}} H_i(B_k) &= \nu_{ij} \ L_{\mathbf{v}} B_j + \frac{\partial \nu_{ij}}{\partial B_k} B_j \ L_{\mathbf{v}} B_k + D_\tau H_i(B_k) \\
&= \nu_{ik}^{\partial} \ L_{\mathbf{v}} B_k + D_\tau H_i(B_k),
\end{aligned}$$

with

$$\nu^{\partial}(B_k) = \nu_{ik}^{\partial} \ \boldsymbol{e}_i \boldsymbol{e}_k^T = \big(\nu_{ik} + \frac{\partial \nu_{ij}}{\partial B_k} B_j\big) \boldsymbol{e}_i \boldsymbol{e}_k^T \tag{41}$$

the components of the tangent reluctivity tensor of the material. The partial Lie derivative $D_\tau H_i(B_k)$ would represent a variation of the magnetic field components H_i under a change of τ, that would not be due to a variation of the field

components B_k. This term accounts thus for a possible explicit dependency of the material law in the design variable τ and the geometrical changes associated to it, independently of the field argument dependency. There is no such dependency in general. The transformations (6) move indeed the interfaces γ^τ but leave by definition material laws unchanged, so that one has

$$D_\tau H_i(B_k) = 0. \tag{42}$$

We can now write successively

$$\begin{aligned} L_{\mathbf{v}} H_i(B_k)\ \boldsymbol{e}_i &= \nu^\partial_{ik}\ L_{\mathbf{v}} B_k\ \boldsymbol{e}_i \\ &= \nu^\partial_{ij}\ L_{\mathbf{v}} B_k\ \boldsymbol{e}_i \boldsymbol{e}_j^T \boldsymbol{e}_k \\ &= \nu^\partial_{ij}\ \boldsymbol{e}_i \boldsymbol{e}_j^T\ L_{\mathbf{v}} B_k\ \boldsymbol{e}_k \\ &= \{\nu^\partial(B_k)\}(L_{\mathbf{v}} B_k\ \boldsymbol{e}_k) \end{aligned}$$

where $\boldsymbol{e}_j^T \boldsymbol{e}_k = \delta_{jk}$ has been used. At the last line, the tangent reluctivity tensor has been written as an operator acting on the vector (actually a 2-form) $L_{\mathbf{v}} B_k\ \boldsymbol{e}_k$.

The vectors $L_{\mathbf{v}} H_i(B_k)\ \boldsymbol{e}_i$ and $L_{\mathbf{v}} B_k\ \boldsymbol{e}_k$ can now be expressed in terms of $L_{\mathbf{v}}\boldsymbol{H}(\boldsymbol{B})$ and $L_{\mathbf{v}}\boldsymbol{B}$ using (38) and (39) to obtain

$$L_{\mathbf{v}}\boldsymbol{H}(\boldsymbol{B}) - (\nabla \mathbf{v})\,\boldsymbol{H}(\boldsymbol{B}) = \{\nu^\partial(B_k)\}\big(L_{\mathbf{v}}\boldsymbol{B} + (\nabla \mathbf{v})^T \boldsymbol{B} - \boldsymbol{B}\,\mathrm{div}\,\mathbf{v}\big). \tag{43}$$

Similarly, one has for inverse material law $\boldsymbol{B}(\boldsymbol{H})$

$$L_{\mathbf{v}}\boldsymbol{B}(\boldsymbol{H}) + (\nabla \mathbf{v})^T \boldsymbol{B}(\boldsymbol{H}) - \boldsymbol{B}(\boldsymbol{H})\,\mathrm{div}\,\mathbf{v} = \{\mu^\partial(H_k)\}\big(L_{\mathbf{v}}\boldsymbol{H} - (\nabla \mathbf{v})\boldsymbol{H}\big), \tag{44}$$

with $\mu^\partial = (\nu^\partial)^{-1}$.

5. Design Velocity Field Computation

There is some freedom in the definition of the mappings (6), and, hence in the choice of an auxiliary flow with velocity $\mathbf{v}$, that represents the shape modification. Once the flow is chosen, the mathematical expression of the velocity field is the Lie derivative

$$\mathbf{v} = \mathbf{L}_{\mathbf{v}} \boldsymbol{x}, \tag{45}$$

of the coordinate vector $\boldsymbol{x} = (x, y, z)$, where $\{x, y, z\}$ are coordinates on E^3.

Various methods for the automatic generation of (45) have been proposed in the literature, using either a geometrical constructive approach such as the isoparametric mapping [25, 26, 27, 28], or an auxiliary structure, such as the boundary displacement method [29, 30, 31] or the fictitious load method [32, 33]. In our approach, which belongs to the first category, we propose a generic computer-aided design (CAD) based method in which mesh nodes are relocalized on perturbed geometrical surfaces thanks to their CAD parametric coordinates [37]. The procedure is illustrated in Fig. 3 for a simple plate with an elliptic hole γ^τ, the considered design variable τ being the major axis of the ellipse. The CAD corresponding to the initial value τ is first meshed, so that the coordinates $\boldsymbol{x}^\tau$ of all nodes in that initial situation are known. The design variable τ is then modified by a small amount $\delta\tau$, leading to a slightly perturbed CAD, and in particular a perturbed surface $\gamma^{\tau+\delta\tau}$, Fig. 3. Mesh nodes lying on

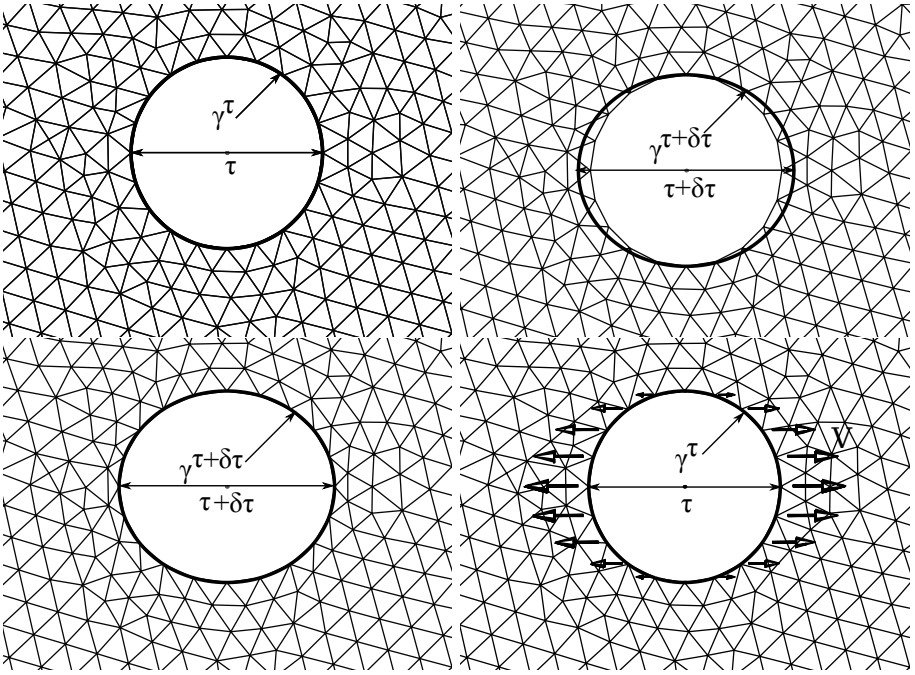

Figure 3: A plate with an elliptic hole γ^τ is considered. The design variable τ is the major axis of the ellipse. After a finite perturbation $\delta\tau$, the mesh nodes lying on the surface γ^τ are relocalized on $\gamma^{\tau+\delta\tau}$ thanks to the CAD parametrization of the surface. The velocity field (46) is approximated by finite difference of the node positions before and after the perturbation.

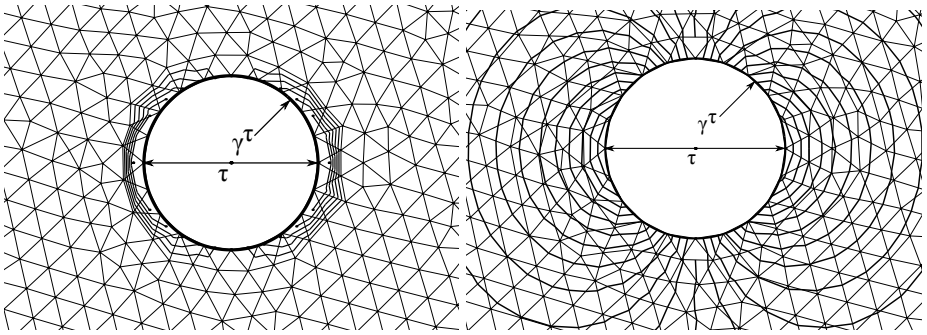

Figure 4: The velocity field (46) so far computed for the mesh nodes lying in the elliptic surface γ^τ, is extended into either a one element thick layer on both sides of the surface γ^τ using the EL method (left), or in the whole domain using a LaS method (right).

γ^τ with coordinates $\boldsymbol{x}^\tau$ can then be relocalized on $\gamma^{\tau+\delta\tau}$ thanks to their parametric coordinates. If $\boldsymbol{x}^{\tau+\delta\tau}$ represent the relocalized coordinates, a discrete approximation of the vector field (45) is given by the finite difference

$$\mathbf{v} \approx \frac{\boldsymbol{x}^{\tau+\delta\tau} - \boldsymbol{x}^\tau}{\delta\tau}, \tag{46}$$

at all nodes on the surface γ^τ.

We however need the velocity field over the whole simulation domain Ω. It is thus extended from the surface γ^τ into Ω by one of the following two methods:

- Laplacian smoothing (LaS) [42]: the velocity field at inner nodes is obtained by solving a scalar Laplace equation for each component of the velocity field, with Dirichlet boundary conditions equal to (46) on γ^τ, and to zero on all other surfaces of the geometrical model. The x-component of the velocity field is illustrated in Fig. 4.

- Element layer (EL) extension: the velocity field is simply interpolated with the nodal shape functions of the initial mesh, assuming nodal values given by (46) at nodes on γ^τ, and equal to zero otherwise. The support of this velocity field is thus limited to a one element thick layer on both side of the surface γ^τ. The x-component of the velocity field for the same example as above is illustrated in Fig. 4.

Comparative convergence [43] diagrams are presented in Fig. 5. The sensitivity of a performance function is computed with first order finite elements for various perturbation step $\delta\tau$ and mesh refinement. It is observed that perturbation steps $\delta\tau$ between 10^{-3} and 10^{-10} are equally valid. A similar convergence rate is obtained with both methods. The main advantage of the LaS method is to generate velocity fields that preserve mesh quality for large perturbations. For sensitivity calculations however, where the perturbation is infinitesimal, the EL approach is to be preferred since it offers the same accuracy at a much lower computational cost. In addition to bypassing the solution of the Laplace equation necessary for the LaS approach, the support of all the volume integrals in sensitivity equations (13), (19), (24) and (26) which involve the velocity field is reduced to the layer of elements connected to the moving interfaces of

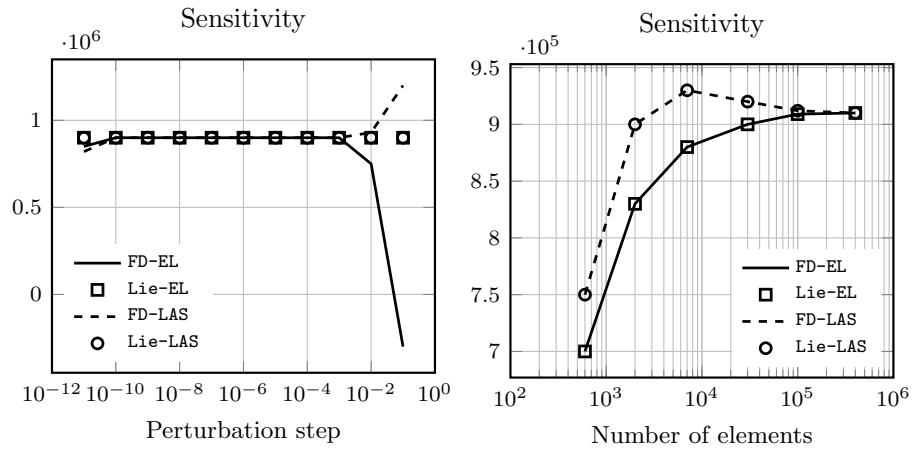

Figure 5: A linear elastic model is defined over the plate, in Fig. 3, where the design variable τ is the major axis of the elliptical hole and the internal energy is the performance function. The sensitivity of the internal energy with respect to τ is computed using a global finite difference (FD) and the Lie derivative (Lie), for which the velocity field obtained through EL method and LaS method is used. Sensitivity based in either EL or LaS exhibits similar convergence rate with respect to perturbation step $\delta\tau$ (where the number of elements in the finite element mesh is set to 10^5) and mesh refinement (where $\delta\tau$ is set to 10^{-6}).

Ω. Compared to classical algorithms, where the volume contributions are expressed directly on the interface γ^τ (via application of the divergence theorem), the proposed approach exhibits much better accuracy and stability, without any significant overhead.

6. Application to Magnetostatics

6.1. Problem formulation

Let us consider the magnetic vector potential $\boldsymbol{A}$ formulation, $\boldsymbol{B} = \mathbf{curl}\,\boldsymbol{A}$, on a bounded domain Ω of the Magnetostatics problem excited by a current density $\boldsymbol{J}$

$$\mathbf{curl}\,\boldsymbol{H}(\boldsymbol{B}) = \boldsymbol{J} \qquad \text{in } \Omega \tag{47}$$

$$\boldsymbol{H}(\boldsymbol{B}) = \nu_{ij} B_j \boldsymbol{e}_i \qquad \text{in } \Omega \tag{48}$$

$$\boldsymbol{A} = 0 \qquad \text{on } \partial\Omega. \tag{49}$$

A homogeneous Dirichlet boundary condition (49) is assumed for the sake of simplicity. In (48), the reluctivity tensor components can be function of $\boldsymbol{B}$ (nonlinear material). The weak formulation of the problem reads [44]: find $\boldsymbol{A}^\star$ in an appropriate function space Z_A^0 verifying (49) such that

$$r(\tau, \boldsymbol{A}^\star, \bar{\boldsymbol{A}}) \equiv \int_\Omega R(\tau, \boldsymbol{A}^\star, \bar{\boldsymbol{A}})\ \mathrm{d}\Omega = 0, \quad \forall \bar{\boldsymbol{A}} \in Z_A^0, \tag{50}$$

with

$$R(\tau, \boldsymbol{A}^\star, \bar{\boldsymbol{A}}) \equiv \boldsymbol{H}(\boldsymbol{B}^\star) \cdot \bar{\boldsymbol{B}} - \boldsymbol{J} \cdot \bar{\boldsymbol{A}}, \tag{51}$$

where $\boldsymbol{B}^\star = \mathbf{curl}\,\boldsymbol{A}^\star$, $\bar{\boldsymbol{B}} = \mathbf{curl}\,\bar{\boldsymbol{A}}$.

6.2. Problem sensitivity analysis

The derivative of the residual (50) at equilibrium with respect to a design variable τ is obtained by applying the chain rule of derivatives,

$$\begin{aligned}\frac{\mathrm{d}}{\mathrm{d}\tau} r(\tau, \boldsymbol{A}^\star, \bar{\boldsymbol{A}}) &= \int_\Omega \Big(L_{\mathbf{v}} \boldsymbol{H}(\boldsymbol{B}^\star) \cdot \bar{\boldsymbol{B}} + \boldsymbol{H}(\boldsymbol{B}^\star) \cdot L_{\mathbf{v}} \bar{\boldsymbol{B}} - L_{\mathbf{v}} \boldsymbol{J} \cdot \bar{\boldsymbol{A}} - \boldsymbol{J} \cdot L_{\mathbf{v}} \bar{\boldsymbol{A}} \Big) \, \mathrm{d}\Omega \\ &= \int_\Omega \Big(L_{\mathbf{v}} \boldsymbol{H}(\boldsymbol{B}^\star) \cdot \bar{\boldsymbol{B}} - L_{\mathbf{v}} \boldsymbol{J} \cdot \bar{\boldsymbol{A}} \Big) \, \mathrm{d}\Omega = 0, \end{aligned} \tag{52}$$

since the fact that $\boldsymbol{B}^\star$ is the solution of (50) implies

$$\int_\Omega \Big(H(\boldsymbol{B}^\star) \cdot L_{\mathbf{v}} \bar{\boldsymbol{B}} - \boldsymbol{J} \cdot L_{\mathbf{v}} \bar{\boldsymbol{A}} \Big) \, \mathrm{d}\Omega = 0,$$

since $L_{\mathbf{v}} \bar{\boldsymbol{A}} \in Z_A^0$.

Using (43), on the one hand, one has

$$L_{\mathbf{v}} \boldsymbol{H}(\boldsymbol{B}^\star) = \nu^\partial L_{\mathbf{v}} \boldsymbol{B}^\star + \nu^\partial \Big((\nabla \mathbf{v})^{\mathbf{T}} \boldsymbol{B}^\star - \boldsymbol{B}^\star \operatorname{div} \mathbf{v} \Big) + (\nabla \mathbf{v}) \, \boldsymbol{H}(\boldsymbol{B}^\star). \tag{53}$$

The current $\boldsymbol{J}$, on the other hand, is a 2-form. Its Lie derivative depends on how current is imposed in the model. If the current I flowing in a conducting region Ω^C of the model is fixed, one has

$$\frac{\mathrm{d}I}{\mathrm{d}\tau} = 0 = \int_{\Omega^C} L_{\mathbf{v}} \boldsymbol{J} \, \mathrm{d}\Omega, \tag{54}$$

and the term $L_{\mathbf{v}} \boldsymbol{J}$ then simply vanishes. If on the other hand the current density is constant, which is the case in our application example, one has $L_{\mathbf{v}} J_i = 0$ and by (39)

$$L_{\mathbf{v}} \boldsymbol{J} = \boldsymbol{J} \operatorname{div} \mathbf{v} - (\nabla \mathbf{v})^{\mathbf{T}} \boldsymbol{J}. \tag{55}$$

Substituting (53) and (55) into (52) yields the linear system to solve for $L_{\mathbf{v}} \boldsymbol{A}^\star$

$$\begin{aligned}\int_\Omega \nu^\partial \, L_{\mathbf{v}} \boldsymbol{B}^\star \cdot \bar{\boldsymbol{B}} \; \mathrm{d}\Omega + \Big[\int_\Omega \Big(\nu^\partial \big((\nabla \mathbf{v})^{\mathbf{T}} \boldsymbol{B}^\star - \boldsymbol{B}^\star \operatorname{div} \mathbf{v} \big) \cdot \bar{\boldsymbol{B}} \\ + (\nabla \mathbf{v}) \, \nu \boldsymbol{B}^\star \cdot \bar{\boldsymbol{B}} - (\boldsymbol{J} \operatorname{div} \mathbf{v} - (\nabla \mathbf{v})^{\mathbf{T}} \boldsymbol{J}) \cdot \bar{\boldsymbol{A}} \Big) \; \mathrm{d}\boldsymbol{\Omega} \Big] = \mathbf{0}, \quad \forall \bar{\boldsymbol{A}} \in \mathbf{Z}_{\mathbf{A}}^{\mathbf{0}}. \end{aligned} \tag{56}$$

The first term in (56) involves the tangent stiffness matrix, which is already known from the computation of $A^\star$, and the bracketed terms make up the partial derivative term $\int_\Omega D_\tau R \, \mathrm{d}\Omega$ of (19).

It is to be noted that (56) is valid for 2D and 3D formulations, and generalizes the methods proposed in [17, 18, 19] that were limited to scalar unknown fields, i.e. to scalar potential 3D formulations or 2D electromagnetic problems.

6.3. Performance function

As a simple example of performance function, we choose the magnetic energy in the airgap $\Omega_f \subset \Omega$, i.e.,

$$f(\tau, \boldsymbol{A}) = \int_{\Omega_f} F(\tau, \boldsymbol{A}) \; \mathrm{d}\Omega, \tag{57}$$

with

$$F(\tau, \boldsymbol{A}) = \frac{1}{2}\nu_0 |\boldsymbol{B}|^2. \tag{58}$$

The correct way to evaluate the Lie derivative of the norm $|\boldsymbol{B}|^2$ is to write it as a scalar product $\boldsymbol{H}(\boldsymbol{B}) \cdot \boldsymbol{B}$ and to invoke (43) in the linear material case this time.

One has then

$$L_{\mathbf{v}} \boldsymbol{H} = \nu_0 \Big(L_{\mathbf{v}} \boldsymbol{B} \Big) + \nu_0 \Big((\nabla \mathbf{v})^T \, \boldsymbol{B} + (\nabla \mathbf{v}) \boldsymbol{B} - \boldsymbol{B} \, \mathrm{div}\, \mathbf{v} \Big),$$

and

$$\frac{\mathrm{d}}{\mathrm{d}\tau} f(\boldsymbol{\tau}, \boldsymbol{A}^\star) = \int_{\Omega_f} \nu_0 \, L_{\mathbf{v}} \boldsymbol{B}^\star \cdot \boldsymbol{B}^\star \, \mathrm{d}\Omega + \Big[\int_{\Omega_f} \frac{\nu_0}{2} \Big((\nabla \mathbf{v})^{\mathbf{T}} \boldsymbol{B}^\star + (\nabla \mathbf{v}) \, \boldsymbol{B}^\star \tag{59}$$
$$- \boldsymbol{B}^\star \, \mathrm{div}\, \mathbf{v} \Big) \cdot \boldsymbol{B}^\star \, \mathrm{d}\Omega \Big],$$

where the first term and the bracketed terms are the Fréchet derivative term and the the partial Lie derivative term $\int_\Omega D_\tau F \, \mathrm{d}\Omega$ of (13), respectively.

6.4. Numerical example

The calculation of the sensitivity is demonstrated with the inductor system depicted in Fig. 6. The system is excited by a fixed current density $\boldsymbol{J}$. The design variable τ is the thickness of the core and the performance function f is chosen as the energy in the airgap (57). The E-core is modeled with either a linear or a nonlinear magnetic material, and both a 2D and a 3D geometrical model are considered.

The EL method has been used to extend the velocity field associated with the perturbation of τ (cf. Section 5), and its nodal values (46) are shown in the bottom pictures in Fig. 6. The support of all volume integrals in (56) and (59) is then limited to one finite element layer on both sides of the moving interfaces.

The sensitivity calculated analytically is compared with that obtained by finite difference with a perturbation step chosen small enough to avoid truncation and condition errors as illustrated in Fig. 7. Convergence diagrams for the sensitivity (with $\delta\tau = 10^{-6}$) of energy and for the energy itself are presented in Figs. 8 and 9. It is first observed that the analytic approach exactly matches the finite difference approach in all cases. Convergence is slower for sensitivity than for energy as the mesh is refined. As expected, convergence is also faster with second order elements. One notices that energy for first order in 3D is clearly not converged as a lot of elements in the airgap are needed. Then sensitivity is not converged yet to the exact value.

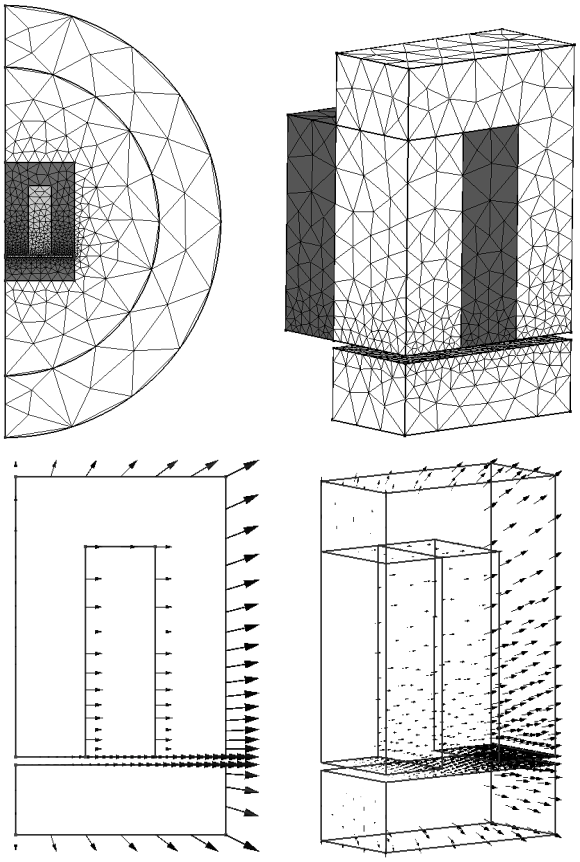

Figure 6: Top: Magnetostatic test case for the sensitivity analysis: inductor with symmetries in 2D (left) and 3D (right) excited by a fixed current density. The design variable τ is the thickness of the magnetic core. Bottom: Nodal values on the boundaries of the velocity field (46) related to the perturbation of τ.

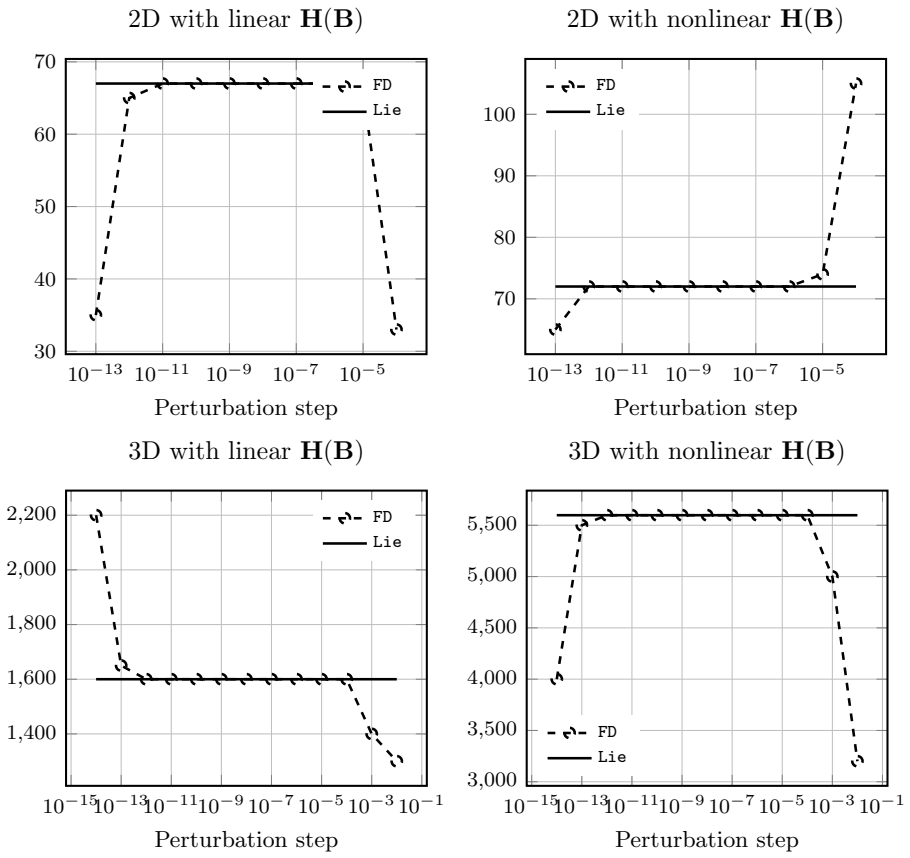

Figure 7: Sensitivity (59) of the inductor energy (evaluated in the airgap) with respect to the magnetic core thickness computed with the finite difference method (FD) and the Lie derivative approach (Lie) for varying perturbation step in 2D (left column) and in 3D (right column). The magnetic core of the inductor is considered as linear in the top while a nonlinear reluctivity is considered in the bottom.

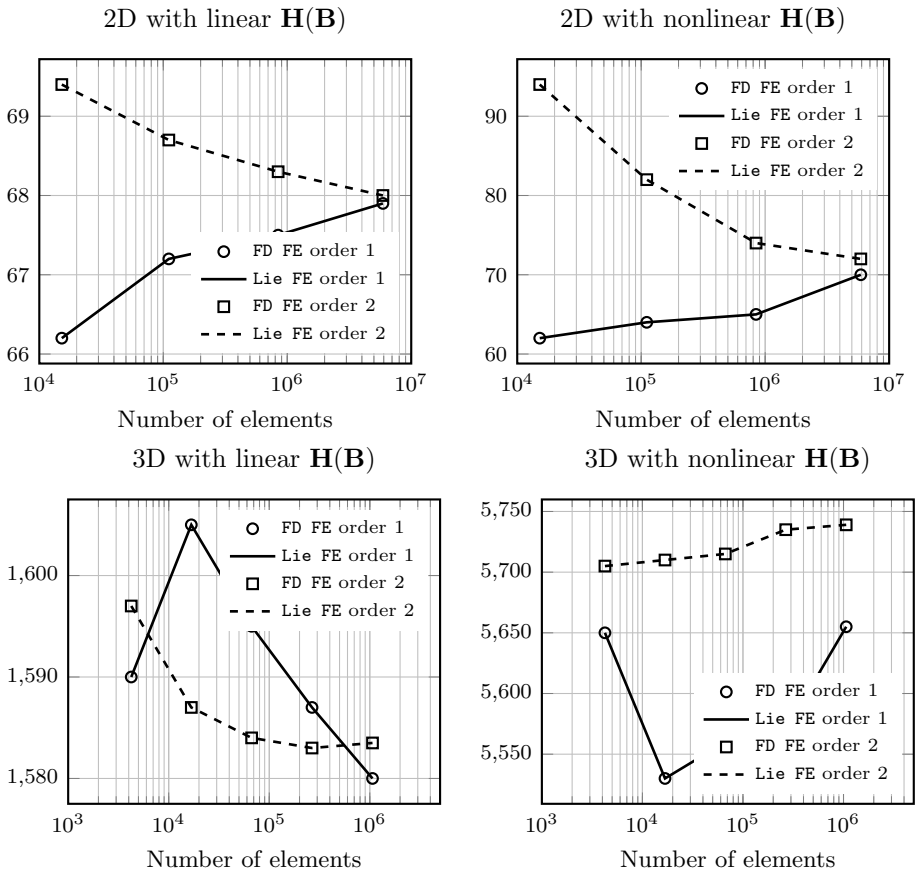

Figure 8: Sensitivity (59) of the inductor energy (evaluated in the airgap) with respect to the magnetic core thickness computed with the finite difference method (FD) and the analytical approach (Lie) for refined mesh with respectively first order (order 1) and second order (order 2) finite elements (FE). The magnetic core of the inductor is considered as linear in the top while a nonlinear reluctivity is considered in the bottom.

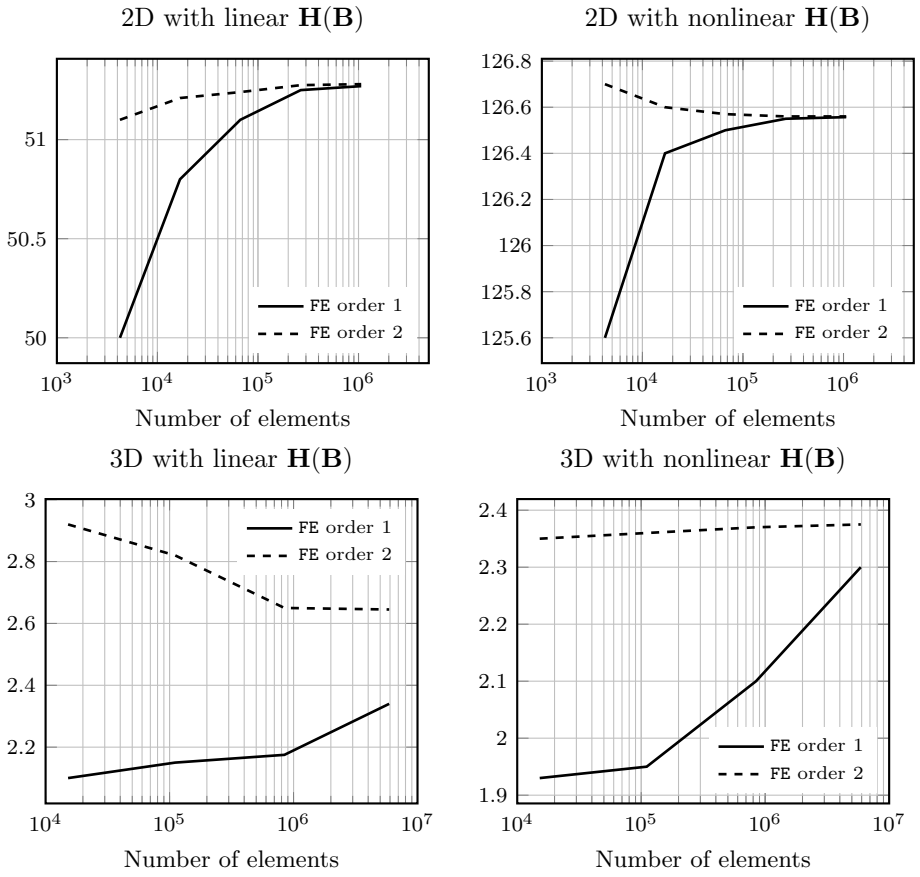

Figure 9: Energy (57) evaluated in the airgap of the inductor, considered in 2D (first column) and 3D (second column) for refined mesh with respectively first (order 1) and second order (order 2) finite elements (FE). The magnetic core of the inductor is considered as linear in the first row while a nonlinear reluctivity is considered in the second row.

7. Application to Linear Elastostatics

7.1. Problem formulation

In linear elasticity, the displacement field $\boldsymbol{u} = u_j \boldsymbol{E}_j$ is expressed in an absolute vector basis $\{\boldsymbol{E}_j, j = 1, 2, 3\}$ of the Euclidean space E^3, whose basis vectors are not affected by the geometrical deformation associated with the variation of τ.

The gradient of the displacement field is the tensor

$$(\nabla \boldsymbol{u}) = (\nabla u_j)\boldsymbol{E}_j^T = \frac{\partial u_j}{\partial x_i}\ \boldsymbol{e}_i \boldsymbol{E}_j^T, \tag{60}$$

and the strain tensor is defined as the symmetrical part of $(\nabla \boldsymbol{u})$,

$$\boldsymbol{\epsilon} = \frac{1}{2}\big((\nabla \boldsymbol{u}) + (\nabla \boldsymbol{u})^T\big) = \epsilon_{ij}\ \boldsymbol{e}_i \boldsymbol{E}_j^T \quad , \quad \epsilon_{ij} = \frac{1}{2}\left(\frac{\partial u_j}{\partial x_i} + \frac{\partial u_i}{\partial x_j}\right). \tag{61}$$

The stress tensor

$$\boldsymbol{\sigma} = \sigma_{ij}\ \boldsymbol{e}_i \boldsymbol{E}_j^T \quad , \quad \sigma_{ij} = \sigma_{ji} \tag{62}$$

is a symmetric tensor obtained from the strain tensor by means of a constitutive relationship

$$\sigma_{ij}(\epsilon_{kl}) = C_{ijkl}\ \epsilon_{kl}. \tag{63}$$

Assuming, for the sake of simplicity, a homogeneous Dirichlet boundary condition, the elasticity problem reads

$$\operatorname{div} \boldsymbol{\sigma}(\boldsymbol{\epsilon}) + \boldsymbol{g} = 0 \qquad \text{in } \Omega, \tag{64}$$

$$\boldsymbol{\sigma}(\boldsymbol{\epsilon}) = C_{ijkl}\ \epsilon_{kl}\ \boldsymbol{e}_i \boldsymbol{E}_j^T \qquad \text{in } \Omega, \tag{65}$$

$$\boldsymbol{u} = 0 \qquad \text{on } \partial\Omega, \tag{66}$$

with $\boldsymbol{g}$ an imposed volume force density. The weak formulation of the problem reads [45]: find $\boldsymbol{u}^\star$ in an appropriate function space Z_u^0 verifying (66) such that

$$r\,(\tau, \boldsymbol{u}^\star, \bar{\boldsymbol{u}}) = \int_\Omega R(\tau, \boldsymbol{u}^\star, \bar{\boldsymbol{u}})\ \mathrm{d}\Omega, \quad \forall \bar{\boldsymbol{u}} \in Z_u^0, \tag{67}$$

with

$$R(\tau, \boldsymbol{u}^\star, \bar{\boldsymbol{u}}) \equiv \boldsymbol{\sigma}(\boldsymbol{\epsilon}^\star) : \nabla \bar{\boldsymbol{u}} - \boldsymbol{g} \cdot \bar{\boldsymbol{u}}, \tag{68}$$

where $\boldsymbol{\epsilon}^\star = \frac{1}{2}((\nabla \boldsymbol{u}^\star) + (\nabla \boldsymbol{u}^\star)^T)$.

7.2. Problem sensitivity analysis

The derivative of the residual (67) at equilibrium is obtained by the chain rule of derivatives

$$\begin{aligned}\frac{\mathrm{d}r}{\mathrm{d}\tau}(\tau, \boldsymbol{u}^\star, \bar{\boldsymbol{u}}) &= \int_\Omega \Big(L_{\mathbf{v}}\boldsymbol{\sigma}(\boldsymbol{\epsilon}^\star) : \nabla \bar{\boldsymbol{u}} + \boldsymbol{\sigma}(\boldsymbol{\epsilon}^\star) : L_{\mathbf{v}}\nabla \bar{\boldsymbol{u}} - L_{\mathbf{v}}\boldsymbol{g} \cdot \bar{\boldsymbol{u}} - \boldsymbol{g} \cdot L_{\mathbf{v}}\bar{\boldsymbol{u}}\Big)\ \mathrm{d}\Omega \\ &= \int_\Omega \Big(L_{\mathbf{v}}\boldsymbol{\sigma}(\boldsymbol{\epsilon}^\star) : \nabla \bar{\boldsymbol{u}} - L_{\mathbf{v}}\boldsymbol{g} \cdot \bar{\boldsymbol{u}}\Big)\ \mathrm{d}\Omega = 0, \end{aligned} \tag{69}$$

since

$$\int_\Omega \Big(\boldsymbol{\sigma}(\boldsymbol{\epsilon}^\star) : L_{\mathbf{v}}\nabla \bar{\boldsymbol{u}} - \boldsymbol{g} \cdot L_{\mathbf{v}}\bar{\boldsymbol{u}}\Big)\ \mathrm{d}\Omega = 0,$$

by (67) because $L_{\mathbf{v}}\bar{\boldsymbol{u}} \in Z_u^0$.

The Lie derivative of the elastic constitutive relationship (65) is evaluated as follows. One first note that

$$L_{\mathbf{v}}\sigma_{ij}(\epsilon_{kl}) = C_{ijkl}(L_{\mathbf{v}}\epsilon_{kl}) + D_\tau\sigma_{ij}(\epsilon_{kl}), \tag{70}$$

where, based on the same argument as above (42), $D_\tau\sigma_{ij}(\epsilon_{kl}) = 0$. It then follows, reintroducing the tensor basis,

$$\begin{aligned}(L_{\mathbf{v}}\sigma_{ij})\boldsymbol{e}_i\boldsymbol{E}_j^T &= C_{ijkl}\ (L_{\mathbf{v}}\epsilon_{kl})\boldsymbol{e}_i\boldsymbol{E}_j^T \\ &= \{C\}\big(L_{\mathbf{v}}\epsilon_{kl}\ \boldsymbol{e}_k\boldsymbol{E}_l^T\big)\end{aligned}$$

where, at the last line, the Hooke tensor has been written as an operator acting on the tensor $L_{\mathbf{v}}\epsilon_{kl}\ \boldsymbol{e}_k\boldsymbol{E}_l^T$. Equation (44) can now be invoked, if one notes that the gradient $\nabla u_j = (\nabla\boldsymbol{u})\boldsymbol{E}_j$ is a 1-form whereas the vector $\sigma_{ij}\boldsymbol{e}_i = \boldsymbol{\sigma}\boldsymbol{E}_j$ is a 2-form. One has by (39) and (38)

$$\begin{aligned}L_{\mathbf{v}}(\boldsymbol{\sigma}\boldsymbol{E}_j) &= (L_{\mathbf{v}}\sigma_{ij})\boldsymbol{e}_i - (\nabla\mathbf{v})^T(\boldsymbol{\sigma}\boldsymbol{E}_j) + (\boldsymbol{\sigma}\boldsymbol{E}_j)\,\mathrm{div}\,\mathbf{v} \\ L_{\mathbf{v}}\big((\nabla\boldsymbol{u})\boldsymbol{E}_j\big) &= L_{\mathbf{v}}\epsilon_{kl}\ \boldsymbol{e}_k + (\nabla\mathbf{v})\big((\nabla\boldsymbol{u})\boldsymbol{E}_j\big),\end{aligned}$$

so that

$$L_{\mathbf{v}}(\boldsymbol{\sigma}\boldsymbol{E}_j)+(\nabla\mathbf{v})^T(\boldsymbol{\sigma}\boldsymbol{E}_j)-(\boldsymbol{\sigma}\boldsymbol{E}_j)\,\mathrm{div}\,\mathbf{v} = \{C\}\Big(L_{\mathbf{v}}\big((\nabla\boldsymbol{u})\boldsymbol{E}_j\big)-(\nabla\mathbf{v})\big((\nabla\boldsymbol{u})\boldsymbol{E}_j\big)\Big),$$

and, after removing the constant and uniform absolute basis vector $\boldsymbol{E}_j$, which are not affected by the geometrical deformation,

$$L_{\mathbf{v}}\boldsymbol{\sigma}(\boldsymbol{\epsilon}) + (\nabla\mathbf{v})^T\boldsymbol{\sigma}(\boldsymbol{\epsilon}) - \boldsymbol{\sigma}(\boldsymbol{\epsilon})\,\mathrm{div}\,\mathbf{v} = \{C\}\big(L_{\mathbf{v}}\nabla\boldsymbol{u} - (\nabla\mathbf{v})(\nabla\boldsymbol{u})\big). \tag{71}$$

Substituting into (69) and noting that $L_{\mathbf{v}}\boldsymbol{g} = 0$ if the resultant force associated with $\boldsymbol{g}$ is independent of τ, one has finally

$$\begin{aligned}&\int_\Omega \{C\}\big(L_{\mathbf{v}}\nabla\boldsymbol{u}^\star\big) : \nabla\bar{\boldsymbol{u}}\ \mathrm{d}\Omega + \Big[\int_\Omega \Big(\,\mathrm{div}\,\mathbf{v}\ \boldsymbol{\sigma}(\boldsymbol{\epsilon}^\star) : \nabla\bar{\boldsymbol{u}} - \{\mathbf{C}\}\big((\nabla\mathbf{v})(\nabla\boldsymbol{u}^\star)\big) : \nabla\bar{\boldsymbol{u}} \\ &\quad - (\nabla\mathbf{v})^{\mathbf{T}}\boldsymbol{\sigma}(\boldsymbol{\epsilon}^\star) : (\nabla\bar{\boldsymbol{u}})\Big)\ \mathrm{d}\boldsymbol{\Omega}\Big] = \mathbf{0}, \quad \forall\bar{\boldsymbol{u}} \in \mathbf{Z_u^0}.\end{aligned} \tag{72}$$

The first term in (72) involves the tangent stiffness matrix of problem (67), while the bracketed terms account for the explicit dependency (i.e. holding the field argument $\boldsymbol{u}$ constant) of the residual on the variation of τ, i.e. $\int_\Omega D_\tau R\,\mathrm{d}\Omega$ as introduced in (19), exactly as obtained in [34].

7.3. Performance function

As a simple example of performance function, we choose the internal energy in the domain Ω, i.e.,

$$f(\tau,\boldsymbol{u}) = \int_\Omega F(\tau,\boldsymbol{u})\ \mathrm{d}\Omega, \tag{73}$$

with

$$F(\tau,\boldsymbol{u}) = \frac{1}{2}\boldsymbol{\sigma}(\boldsymbol{\epsilon}) : \boldsymbol{\epsilon}. \tag{74}$$

The derivative of the performance function (73) is now obtained similarly to the derivative of the residual (69), by recalling the Lie derivative of the stress tensor (71),

$$\frac{\mathrm{d}}{\mathrm{d}\tau} f(\tau, \boldsymbol{u}^\star) = \int_\Omega \boldsymbol{\sigma}\Big(\nabla(L_{\mathbf{v}}\boldsymbol{u}^\star)\Big) : \nabla \boldsymbol{u}^\star \ \mathrm{d}\Omega + \Big[\frac{1}{2}\int_\Omega \Big(\operatorname{div}\mathbf{v}\ \boldsymbol{\sigma}(\boldsymbol{\epsilon}^\star) : \nabla \bar{\boldsymbol{u}} - \boldsymbol{\sigma}\big((\nabla\mathbf{v})(\nabla \boldsymbol{u}^\star)\big) : \nabla \bar{\boldsymbol{u}} - \boldsymbol{\sigma}(\boldsymbol{\epsilon}^\star) : \big((\nabla\mathbf{v})(\nabla \bar{\boldsymbol{u}})\big)\Big)\ \mathrm{d}\boldsymbol{\Omega}\Big], \tag{75}$$

where the first term in (75) is the Fréchet derivative of the performance function with respect to the unknown field $\boldsymbol{u}$, while the bracketed terms are the explicit dependency (i.e. holding the field argument $\boldsymbol{u}$ constant) of f on the variation of τ, i.e. $\int_\Omega D_\tau F \,\mathrm{d}\Omega$ as introduced in (13).

7.4. Numerical example

The calculation of the sensitivity is demonstrated with the infinite plate with an elliptic hole depicted in Fig. 10. The system is excited by a biaxial load of fixed magnitude. The design variable τ is the major axis of the ellipse and the performance function f is chosen as the energy in the plate (73). The plate is made a linear elastic steel, and both a 2D and a 3D geometrical model are considered.

The EL method has been used, similarly to the inductor system (cf. Fig. 6), to extend the velocity field associated with the perturbation of τ (cf. Section 5), and its nodal values (46) are shown in the bottom pictures in Fig. 10. The support of all volume integrals in (72) and (75) is then limited to one finite element layer on both sides of the moving interfaces.

The sensitivity calculated analytically is compared with that obtained by finite difference with a perturbation step chosen small enough to avoid truncation and condition errors as illustrated in the top of Fig. 11. Convergence diagrams for the sensitivity (with $\delta\tau = 10^{-6}$) and the internal energy are presented in Figs. 11 and 12. All the conclusions obtained for the Magnetostatic numerical example (cf. Section 6) still hold here.

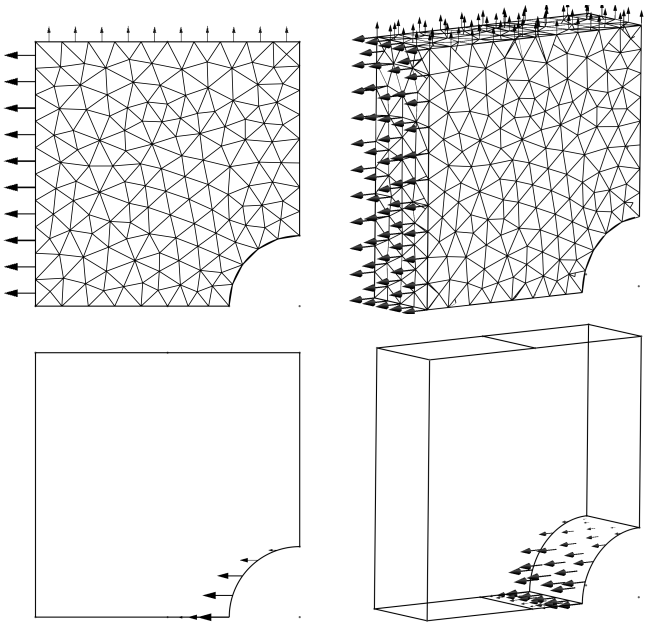

Figure 10: Top: Elasticity test case for the sensitivity analysis: infinite plate with symmetries in 2D (left) and 3D (right) excited by a biaxial load. The design variable τ is the major axis of the elliptic hole. Bottom: Nodal values on the boundaries of the velocity field (46) related to the perturbation of τ.

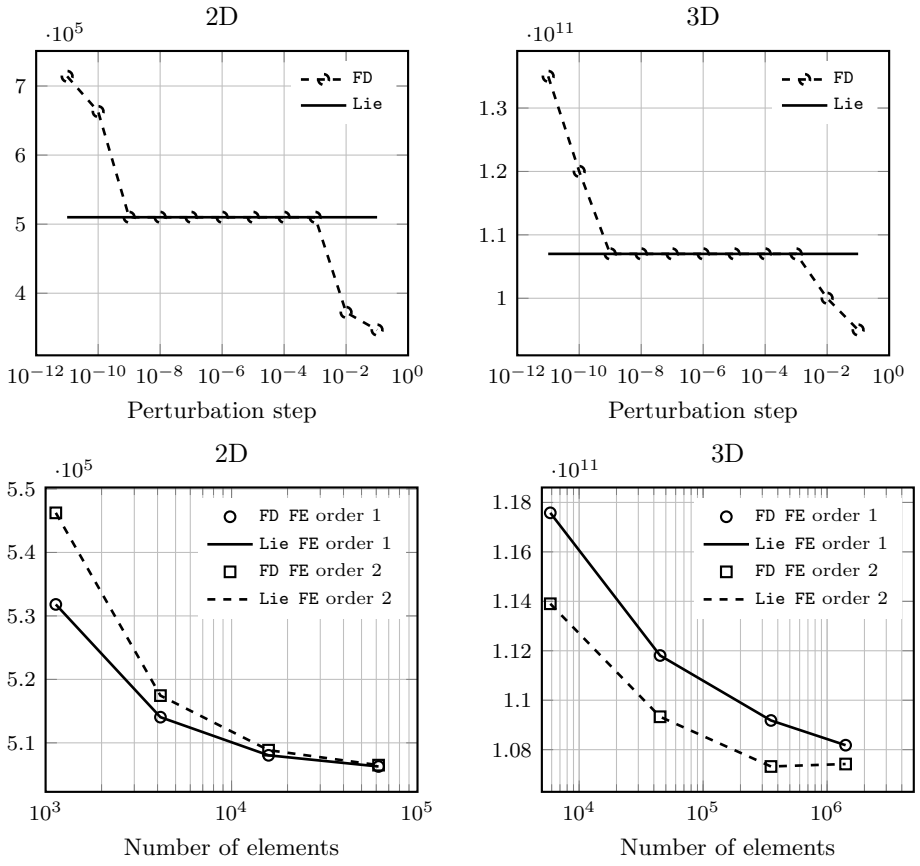

Figure 11: Sensitivity (75) of the plate compliance (internal energy) with respect to the elliptical hole major axis length computed with the finite difference method (FD) and the Lie derivative approach (Lie). Top: the perturbation step is varied in 2D (left column) and 3D (right column). The sensitivity based on the Lie derivative doesn't suffer from the truncation and conditions errors proper to the FD then the choice of the perturbation step is not critical. Bottom: the mesh is refined and the convergence is studied with respectively first (order 1) and second (order 2) order finite elements (FE). Both methods converge to the same result when the mesh is refined, with a faster convergence for second order finite elements.

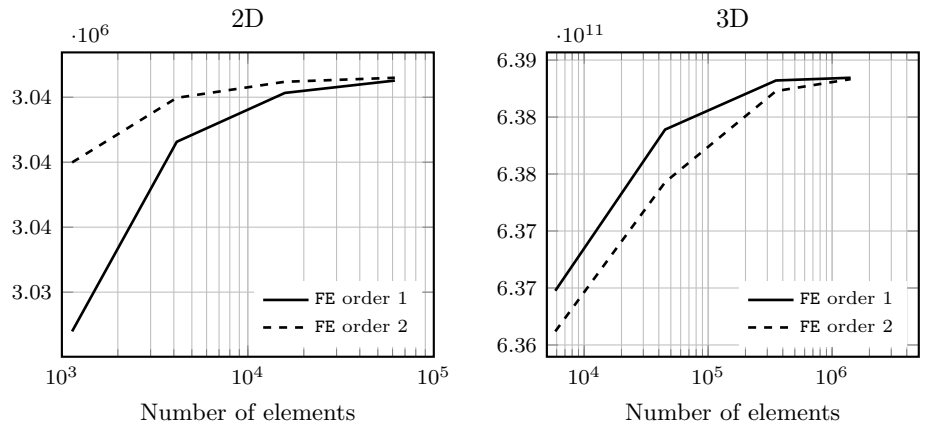

Figure 12: Internal energy (73), considered in 2D (left) and 3D (right) for refined mesh with respectively first (order 1) and second order (order 2) finite elements (FE).

8. Conclusion and perspectives

The shape sensitivity of a performance function can be expressed analytically as a Lie derivative. Related differential geometry concepts are introduced in this paper and reformulated with conventional tensor and vector analysis notations. Theoretical formulas for shape sensitivity are derived in detail, following both the direct and the adjoint approach. The obtained formulas have a rather large number of terms, which can however either be reused from the finite element solution or evaluated on a support limited to a one layer thick layer of finite elements on both sides of the surfaces involved in the shape variation. A number of results previously obtained by other authors with a classical vector calculus approach in the area of structural mechanics and scalar magnetostatics are recovered with the proposed framework, which is however more general.

Numerical examples in nonlinear magnetostatics and linear elasticity have been presented, and validated with the finite difference approach. Convergence of the computed sensitivity with mesh refinement have been studied with first and second order elements. An efficient method for the construction of the design velocity field has been described, which allows to complete a general automatic sensitivity computation tool.

The theoretical results gathered in this paper pave the way towards more involved applications, such as eddy current problems, and multiphysics problems.

Acknowledgments

This work was supported in part by the Walloon Region of Belgium under grant RW-1217703 (WBGreen FEDO) and the Belgian Science Policy under grant IAP P7/02.

References

[1] O. Zienkiewicz, J. Campbell, Shape optimization and sequential linear programming, Optimum structural design (1973) 109–126.

[2] A. Francavilla, C. Ramakrishnan, O. Zienkiewicz, Optimization of shape to minimize stress concentration, The Journal of Strain Analysis for Engineering Design 10 (2) (1975) 63–70.

[3] R. Fox, Constraint surface normals for structural synthesis techniques, AIAA Journal 3 (8) (1965) 1517–1518.

[4] L. A. Schmit, Structural design by systematic synthesis, in: Proceedings of the Second ASCE Conference on Electronic Computation, 1960, pp. 105–122.

[5] C. Fleury, L. A. Schmit Jr, Dual methods and approximation concepts in structural synthesis, NASA (1980) CR–3226.

[6] K. Svanberg, The method of moving asymptotes- a new method for structural optimization, International journal for numerical methods in engineering 24 (2) (1987) 359–373.

[7] Y. Nesterov, A. Nemirovskii, Y. Ye, Interior-point polynomial algorithms in convex programming, Vol. 13, SIAM, 1994.

[8] H. M. Adelman, R. T. Haftka, Sensitivity analysis of discrete structural systems, AIAA journal 24 (5) (1986) 823–832.

[9] J. S. Arora, E. J. Haug, Methods of design sensitivity analysis in structural optimization, AIAA journal 17 (9) (1979) 970–974.

[10] G. Allaire, F. Jouve, A.-M. Toader, Structural optimization using sensitivity analysis and a level-set method, Journal of computational physics 194 (1) (2004) 363–393.

[11] K. Dems, Z. Mroz, Variational approach by means of adjoint systems to structural optimization and sensitivity analysis -II: Structure shape variation, International Journal of Solids and Structures 20 (6) (1984) 527–552.

[12] R. Haber, Application of the eulerian-lagrangian kinematic description to structural shape optimization, in: Proceedings of NATO ASI Computer-Aided Optimal Design, 1986, pp. 297–307.

[13] E. J. Haug, J. S. Arora, Applied optimal design: mechanical and structural systems, Wiley, 1979.

[14] U. Kirsch, Optimum structural design: concepts, methods, and applications, McGraw-Hill, 1981.

[15] V. Komkov, K. K. Choi, E. J. Haug, Design sensitivity analysis of structural systems, Vol. 177, Academic press, 1986.

[16] R. T. Haftka, Z. Gürdal, Elements of structural optimization, Vol. 11, Springer Science & Business Media, 2012.

[17] J. Biedinger, D. Lemoine, Shape sensitivity analysis of magnetic forces, Magnetics, IEEE Transactions on 33 (3) (1997) 2309–2316.

[18] C.-S. Koh, S.-Y. Hahn, K.-S. Lee, K. Choi, Design sensitivity analysis for shape optimization of 3-D electromagnetic devices, Magnetics, IEEE Transactions on 29 (2) (1993) 1753–1757.

[19] I.-H. Park, J.-L. Coulomb, S.-Y. Hahn, Implementation of continuum sensitivity analysis with existing finite element code, Magnetics, IEEE Transactions on 29 (2) (1993) 1787–1790.

[20] B. Schutz, Geometrical methods of mathematical Physics, Cambridge University Press, 1980.

[21] F. W. Warner, Foundations of differentiable manifolds and Lie groups, Graduate texts in mathematics, Springer-Verlag, New York, 1983.

[22] R. Bishop, S. Goldberg, Tensor analysis on manifolds, Macmillan, 1968.

[23] T. Frankel, The geometry of physics: an introduction, Cambridge University Press, 1997.

[24] F. Henrotte, Handbook for the computation of electromagnetic forces in a continuous medium, Int. Compumag Society Newsletter 24 (2) (2004) 3–9.

[25] M. Botkin, Shape optimization of plate and shell structures, AIAA Journal 20 (2) (1982) 268–273.

[26] V. Braibant, C. Fleury, Shape optimal design using b-splines, Computer Methods in Applied Mechanics and Engineering 44 (3) (1984) 247–267.

[27] R. Yang, M. Botkin, A modular approach for three-dimensional shape optimization of structures, AIAA journal 25 (3) (1987) 492–497.

[28] M. H. Imam, Three-dimensional shape optimization, International Journal for Numerical Methods in Engineering 18 (5) (1982) 661–673.

[29] K. K. Choi, Shape design sensitivity analysis and optimal design of structural systems, Springer, 1987.

[30] K. K. Choi, T.-M. Yao, On 3-D modeling and automatic regridding in shape design sensitivity analysis, NASA Conference Publication 2457 (1987) 329–345.

[31] T.-M. Yao, K. K. Choi, 3-D shape optimal design and automatic finite element regridding, International Journal for Numerical Methods in Engineering 28 (2) (1989) 369–384.

[32] A. Belegundu, S. Rajan, A shape optimization approach based on natural design variables and shape functions, Computer Methods in Applied Mechanics and Engineering 66 (1) (1988) 87–106.

[33] S. Zhang, A. Belegundu, A systematic approach for generating velocity fields in shape optimization, Structural and Multidisciplinary Optimization 5 (1) (1992) 84–94.

[34] N. H. K. Kyung K. Choi, Structural Sensitivity Analysis and Optimization 1, Springer Science & Business Media, Inc., 2005.

[35] Il-Han Park, J. L. Coulomb, Song-yop Hahn, Design sensitivity analysis for nonlinear magnetostatic problems by continuum approach, J. Phys. III France 2 (11) (1992) 2045–2053.

[36] D.-H. Kim, S.-H. Lee, I.-H. Park, J.-H. Lee, Derivation of a general sensitivity formula for shape optimization of 2-d magnetostatic systems by continuum approach, Magnetics, IEEE Transactions on 38 (2) (2002) 1125–1128.

[37] C. Geuzaine, J.-F. Remacle, Gmsh: A 3-D finite element mesh generator with built-in pre-and post-processing facilities, International Journal for Numerical Methods in Engineering 79 (11) (2009) 1309–1331.

[38] P. Dular, C. Geuzaine, A. Genon, W. Legros, An evolutive software environment for teaching finite element methods in electromagnetism, IEEE Transactions on Magnetics 35 (3) (1999) 1682–1685.

[39] C. Fleury, Conlin: an efficient dual optimizer based on convex approximation concepts, Structural Optimization 1 (2) (1989) 81–89.

[40] K. Svanberg, A class of globally convergent optimization methods based on conservative convex separable approximations, SIAM Journal on Optimization (2002) 555–573.

[41] E. Kuci, C. Geuzaine, P. Dular, P. Duysinx, Shape optimization of interior permanent magnet motor for torque ripple reduction, in: Proceedings of the 4th International Conference on Engineering Optimization, 2014, p. 187.

[42] P. Duysinx, W. Zhang, C. Fleury, Sensitivity analysis with unstructured free mesh generators in 2-d shape optimization, in: Proceedings of Structural Optimization 93, The World Congress on Optimal Design of Structural Systems, Vol. 2, Structural Optimization, 1993, pp. 205–2012.

[43] R. T. Haftka, B. Barthelemy, On the accuracy of shape sensitivity, Structural optimization 3 (1) (1991) 1–6.

[44] A. Bossavit, Computational electromagnetism: variational formulations, complementarity, edge elements, Academic Press, 1998.

[45] C. Zienkiewicz, R. L. Taylor, The finite element method Vol. 1: Basic formulation and linear problems, no. 3 in finite element method series, Wiley, 1990.